A Narrowband Level Set Method Applied to EIT in Brain for Cryosurgery Monitoring

Soleimani, Manuchehr and Dorn, Oliver and Lionheart, William RB

2006

MIMS EPrint: **2015.79**

Manchester Institute for Mathematical Sciences

School of Mathematics

The University of Manchester

A Narrowband Level Set Method Applied to EIT in Brain for Cryosurgery Monitoring

Manuchehr Soleimani, Oliver Dorn, William R.B. Lionheart

Manuchehr soleimani is with William Lee Innovation centre, School of Materials, The university of Manchester, Manchester M60 1QD, UK, m.soleimani@umist.ac.uk

Abstract

In this paper we investigate the feasibility of applying a novel level set reconstruction technique to electrical imaging of the human brain. We focus particularly on the potential application of Electrical Impedance Tomography (EIT) to cryosurgery monitoring. In this application, cancerous tissue is treated by a local freezing technique using a small needle-like cryosurgery probe. The interface between frozen and non-frozen tissue can be expected to have a relatively high contrast in conductivity and we treat the inverse problem of locating and monitoring this interface during the treatment. A level set method is used as a powerful and flexible tool for tracking the propagating interfaces during the monitoring process. For calculating sensitivities and the Jacobian when deforming the interfaces we employ an adjoint formula rather than a direct differentiation technique. Particulary we are using a narrowband technique for this procedure. This combination of an adjoint technique and a narrowband technique for calculating Jacobians results in a computationally efficient and extremely fast method for solving the inverse problem. Moreover, due to the reduced number of unknowns in each step of the narrowband approach compared to a pixel- or voxel-based technique, our reconstruction scheme tends to be much more stable. We demonstrate that our new method also outperforms its pixel-/ voxel-based counterparts in terms of image quality in this application.

1

Index term- Level set method, shape reconstruction, inverse boundary value problem, Electrical

Impedance Tomography, brain imaging, cryosurgery.

1 Introduction

Electrical impedance tomography (EIT) has been applied to the detection of epileptic seizures [1],

functional brain activity triggered by external stimuli [16], and internal cortical hemorrhage [4],

conditions that all cause local and temporal conductivity changes in brain tissue. In this paper we

are interested in the use of EIT for monitoring cryosurgery [18, 9], a technique that uses freez-

ing to destroy tumorous tissues. We focus on the human head which contains tissues with highly

discontinuous conductivity coefficients. There has been growing interest recently in many appli-

cations in the development and use of geometrical inversion methods, which move away from the

goal of estimating a spatial function represented as pixel or voxel values to concentrate processing

resources instead directly on the recovery of information regarding hidden anomalies. This ap-

proach appears to be promising in brain imaging during a cryosurgery treatment, due to the high

contrast of electrical parameters between frozen tissue and the surrounding tissue. In this paper we

will reformulate the problem of the conductivity reconstruction as an inverse problem for a special

geometrical representation of embedded objects. For the purpose of numerically describing the

boundaries of these objects we employ a level set technique.

The level set technique was initially introduced for tracking propagating interfaces [14], [23],

and more recently it has found applications also in shape reconstruction problems and in image pro-

cessing [7], [11], [22]. In our approach, we employ an iterative method using an update formula for a level set function in each step. Using iteration steps the difference between the simulated and measured data can be minimized. It is assumed that the background distribution and approximate values of the electrical parameters inside the inclusions are known, but that the number, topology and shapes of the inclusions are unknown and have to be recovered from the data. Compared to the more commonly used voxel-based reconstruction schemes, the shape reconstruction approach has the advantage that available prior information about the high parameter contrast of the inclusions compared to the background is incorporated explicitly in the modeling of the problem. In nonlinear voxel-based reconstruction schemes [16], the approximate locations of the unknown obstacles are found easily during the early iterations of the scheme. However, it takes a large number of additional iterations in order to actually build up this high contrast to the background and therefore improve even the information of the correct size of the hidden object.

We will see that, by using the level set technique, rapid convergence to the correct shape and size of the hidden objects can be achieved. This holds true even in situations where we only know approximate values for the contrast provided that these values are still sufficiently different from the background values.

An interesting front tracking method has been studied earlier for a two-dimensional EIT problem applied to a cryosurgery model [19] using a geometrical model of the ice fronts. A so-called 'direct differentiation technique' was employed in that work in order to calculate Jacobian, whereas we employ a more efficient adjoint scheme for this purpose. Moreover, it is well-known that the

level set method has the major advantage that it automatically tracks splitting and merging of objects, and that it has no problems if complicated geometries build up. This might occur for example when multiple probes are used during the treatment. Detecting such more complicated geometries cause no additional problems when employing a level set technique, whereas most alternative shape-modeling techniques require a complicated and cumbersome re-meshing procedure.

In this paper we present a thorough feasibility study of the level set method for the cryosurgery monitoring using a three dimensional head shaped model. We will present fully 3D reconstructions from simulated 3D data.

2 Forward problem

The forward problem in EIT consists of an electrostatic approximation of Maxwell's equations. The fundamental unknown of the forward problem is the electric potential u. Given the conductivity distribution σ in EIT, u is calculated in the domain of interest Ω by solving the partial differential equation

$$\nabla \cdot \sigma \nabla u = 0 \tag{1}$$

with suitable boundary conditions on $\partial \Omega$. Here σ is electrical conductivity coefficients. The equation (1) is solved in conjunction with the set of boundary conditions prescribed by the so-called complete electrode model. Specifically, the boundary current density satisfies,

$$\int_{e_l} \sigma \frac{\partial u}{\partial \hat{n}} = I_l \quad on \quad \Gamma_1, \tag{2}$$

4

$$\sigma \frac{\partial u}{\partial \hat{n}} = 0 \quad on \quad \Gamma_2, \tag{3}$$

whilst for the boundary electric potential measurements, the relation,

$$u + z_l \sigma \frac{\partial u}{\partial \hat{n}} = V_l \quad on \quad \Gamma_1, \tag{4}$$

is valid. Here, I_l denotes the current on the surface of the lth electrode, e_l, V_l is the electric potential measured by e_l, z_l is the associated contact impedance and $\hat{n}$ is the outward-pointing unit normal vector. We use EIDORS-3D [17] in order to solve the forward problem of 3D EIT, and also a modification of EIDORS-3D which is designed to speed up forward calculations [25].

We use the linearized sensitivity of the voltage measurement to a change in electric conductivity in EIT. This type of perturbation calculation, which mathematically amounts to calculating the Fréchet derivative of the measurement data with respect to conductivity, is standard in a broad class of inverse problems (for general form of sensitivity derivation see [8] and derivation of sesitivity formula in EIT see [3], [17]). We will employ an adjoint technique for calculating these sensitivities. Here, at each point in the domain the calculated sensitivity is essentially proportional to the inner product of two electric field vectors $\mathcal{E}_i \cdot \mathcal{E}_j$ at the given location. In particular, we have for EIT

$$\frac{dV_{ij}}{d\sigma} \delta\sigma = -\int_\Omega \delta\sigma \, \mathcal{E}_i \cdot \mathcal{E}_j \, dv \tag{5}$$

Here, Ω is the perturbed region and $\mathcal{E}_i$ and $\mathcal{E}_j$ are the calculated electric fields of the forward problem when electrodes i and j are excited. This sensitivity formula results in an efficient method for the assembly of the Jacobian matrix. In the finite element (FEM) model used in our numerical

experiments, we have $\mathcal{E} = -\nabla u$. We will see further below that also in our shape reconstruction framework these sensitivities will play a central role.

3 Inverse interface problem using level sets

A comprehensive study of our level set technique in the general application of electrical resistance and capacitance imaging has been given in [24]. Therefore, we restrict ourselves here to describe the main features of this technique briefly. Compared to the more typical pixel or voxel based reconstruction schemes, the shape reconstruction approach has the advantage that a priori information about the high contrast of the inclusions is incorporated explicitly in the modelling of the problem. With this technique, a more accurate reconstruction of the high contrast objects can be achieved than is possible with the more traditional reconstruction schemes such as generalized Tikhonov, which have the side-effect of artificially smoothing the reconstructed images. Therefore, these schemes are not well-suited for reconstructing high contrast objects with sharp boundaries. An alternative is to use total variation regularization (TV) [2, 5, 13], a voxel based approach which allows jump changes. But voxel based TV methods are more computationally costly than generalized Tikhonov regularization with a smooth penalty term. Also the use of a Mumford-Shah functional has been proposed in the literature [21]. Level set approaches for general electrical impedance tomography problems have been discussed for example in [10, 6, 24].

In the level set approach, the shape is represented by a higher order function (level set function) [11, 14, 23], which is then used for numerically tracking the changing shapes. One main advantage

6

of this technique is its ability to easily model topological changes of the shapes.

In the level set technique, the boundaries of the shapes are represented by the zero level set of a level set function f. More specifically, if D is the inclusion with conductivity (or permittivity) σ_{int} embedded in a background with conductivity (or permittivity) σ_{ext}, the boundary of the inclusion, which is also an interface between two materials, is given by

$$\partial D := \{r : f(r) = 0\} \tag{6}$$

where the image parameter (assuming $\sigma_{int} < \sigma_{ext}$) at each point r is

$$\sigma(r) = \begin{cases} \sigma_{int} & \{r : f(r) < 0\} \\ \sigma_{ext} & \{r : f(r) > 0\} \end{cases} \tag{7}$$

If we change this level set function for example by adding an update, we move the shapes accordingly. This relation is used in the level set technique when constructing updates δf to a given level set function f such that the shapes are deformed in a way which reduces a given cost function. Fig. 1 shows the level set representation of the shape and a deformation by a perturbation (update) of the level set function. In the figure a velocity function F in the normal direction to the current boundary of the shape S is indicated whose effective propagation in one time step is modeled by a corresponding update δf of the level set function.

The general idea of a regularized Gauss-Newton approach has been combined with our newly developed shape based inversion technique. Using optimization strategies for the shape inversion

7

as an alternative to a shape evolution approach was already suggested in the early paper by Santosa [22]. In order to mathematically derive this new optimization scheme for our situation, we will denote the mapping which assigns to a given level set function f_D the corresponding parameter distribution σ by $\sigma = \Phi(f_D)$. The parameter distribution σ has the same meaning as in the traditional Gauss-Newton inversion scheme. The only difference is that in the shape based situation it is considered as having only two values, namely an interior value and an exterior value. (Certainly, this assumption can be generalized by allowing these interior and exterior values to be smoothly varying functions, separated by the interface. We will not consider this extension here.) Moreover, in our new approach it will only be an intermediate parameter, linking the data finally to the new basic unknown of the inverse problem, namely the level set function f_D.

Having defined this mapping Φ, we can now replace the iterated parameter σ_n by $\sigma_n = \Phi(f_{D^n}) = \Phi(f^n)$. Instead of the classical pixel/voxel based forward mapping $A(\sigma)$ we need to consider now in the new Gauss-Newton type approach the combined mapping

$$B(f) = A(\Phi(f)).$$

If we perturb the latest best guess for the level set function f by some small correction δf, the linearized response in the data will be

$$B'[f]\delta f = A'[\Phi(f)]\Phi'[f]\delta f \tag{8}$$

according to the chain rule. Plugging this into a Gauss-Newton type algorithm, and using an update formula for the level set function as it was derived and discussed in [24], we try to calculate

successive updates δf for the level set function such that the shape corresponding to the final level set function fits the simulated measurements to the given data as accurately as possible.

In [22] Santosa has shown that the linearized infinitesimal response in the parameter due to a perturbation in the level set function can be formally described as

$$\Phi'[\Psi]\delta\Psi = -(\gamma_{\text{int}} - \gamma_{\text{ext}})\frac{\delta\Psi}{|\nabla\Psi|}\delta_{\partial D} \tag{9}$$

where $\delta_{\partial D}$ is the Dirac delta function concentrated on the boundary of the latest best guess for the shape D. The singular nature of the Dirac delta function which is involved in this expression causes some mathematical complications when directly applying this expression to the Gauss-Newton update. (The main difficulty is that the Dirac delta function is not a member of the usually employed Hilbert space L_2.) However, these technical subtleties can be circumvented by approximating the Dirac delta function by a smeared-out version of it (which in fact will now be a member of the space L_2). We will use for this purpose the function

$$\delta_{\partial D}(x) \approx C_\rho\chi_\rho(x)$$

where χ_ρ is the indicator function of a small narrow band of half-width ρ centred at ∂D, and C_ρ is the corresponding normalization factor. With this approximation, we get

$$\Phi'[\Psi]\delta\Psi \approx -(\gamma_{\text{int}} - \gamma_{\text{ext}})\frac{\delta\Psi}{|\nabla\Psi|}C_\rho\chi_\rho(x). \tag{10}$$

It is convenient to further approximate $|\nabla\Psi| \approx c_1$ with some constant c_1, which usually is justified if we rescale our level set function after each step, or even recalculate it as a signed-distance function

9

repeatedly. We finally arrive at

$$\Phi'[\Psi]\delta\Psi \approx a\chi_\rho(x)\delta\Psi \tag{11}$$

with the constant

$$a = -\frac{\gamma_{int} - \gamma_{ext}}{c_1}C_\rho.$$

We denote the discretized form of $\Phi'[\Psi]$ by K, and the Jacobian of G by B. Then, the new Gauss-Newton update is

$$\Psi_{n+1} = \Psi_n + \lambda \left(B_n^T B_n + \alpha^2 L^T L\right)^{-1} B_n^T \left(M - G\left(\Psi_n\right)\right) \tag{12}$$

with

$$B = JK, \qquad B^T = K^T J^T, \qquad B^T B = K^T J^T JK. \tag{13}$$

Notice that (13) implies that $B^T B$ can be restricted to be defined only on the narrow band, since both K and K^T contain discretized versions of $\chi_\rho(x)$.

As a technical subtlety we mention that we apply a narrow-band technique for approximating our interfaces between different domains. This means that during the evolution the interfaces between the subregions are practically 'smeared-out' over a small neighborhood ('narrowband') centered at the interface. Practically, we have to approximate a Dirac Delta function arising in (8) which is concentrated at the boundary of the shape by a characteristic function of the narrowband around this boundary. With this technique, the explicit use of interface conditions for calculating shape sensitivities is avoided.

4   Result and discussion

First of all we consider a simple 2D example. Fig. 2 shows original (a) and reconstruction (b) of multiple objects using the level set method. The background conductivity is 1 Siemens per meter (S/m) and the conductivity inside the inclusions is 10^{-3} S/m. The total number of pixels used in the example are 1945 pixels. In Fig. 3 we have plotted the singular values of the linearized problems which arise in each step when a pixel-based reconstruction method is used and have compared that to the condition number of our shape-based approach using a narrow-band technique. Due to the reduced size of the linearized sub-problems the condition number is much better behaved in a given step of our shape-based scheme than it is in the pixel-based scheme. The number of unknowns in the pixel-based scheme and in the shape-based scheme in each of these linearized subproblems is displayed and compared in Fig. 4.

In our next numerical experiment, we are interested in evaluating changes in the voltage measurements induced by the presence of a spherical frozen region in the brain (see [20], [18].) We solve the complete electrode forward problem on a finite element mesh with 9,063 nodes and 44,304 elements. We use the conductivity coefficients as given in Table 1, which are typical values in this application. Next, we add into the domain an frozen region with conductivity 10^{-5} S/m, and with diameter 15 mm. A total of sixteen electrodes are used and an opposite current pattern of 1 mA is applied. The arrangement of the surface electrodes is shown in Fig. 5, where the frozen area is centered at the point $(100, 100, 100)$ mm.

Fig. 6 shows the voltage differences between several electrodes (see Fig. 5) when the current

11

source and sink electrodes are those numbered 3 and 10 in figure 5. We observe that the voltage difference increases almost linearly with the volume of the frozen area. A similar observation has been reported in [20]. The measured voltages for the other electrodes exhibit the same behavior and are in range of mv, which is practically detectable. Fig. 7 shows the saturation property for the voltage difference when the conductivity of a region decreases or increases. When a certain threshold is reached, an increase (decrease) of conductivity is practically not reflected anymore in the data. From this behavior we conclude that the treatment of the underlying inverse problem as a shape reconstruction problem is justified. This also shows that the reconstruction of the absolute conductivity values (using image based method) will be very hard task both numerically and experimentally (saturation plot means that the voltage differences between two points in very low or very high conductivity is very small).

Fig. 8 shows an example where the evolution of the shape has been tracked by the level set method. The location of the inclusion was recovered after 12 iterations for the first ice-ball size. (the initial guess was 2 cm away from the true object), then we increase the volume of the ice-ball by 10 percent in each step, which requires three or four more iteration steps for the reconstruction. During this evolution we monitor the cost functional which is the least squares difference between estimated voltages and the measured voltages. This gives us a stopping criterion for our shape evolution. Fig. 8 shows two different steps of the first part of our reconstruction, namely the initial shape and the shape after 10 iterations. We find that using the final solution to the previous time step as the initial guess for the current time step reduces the number of necessary iterations

considerably In Fig. 8.c we display cross sections of the reconstructed ice-ball where the true inclusion has a diameter of 15 mm with an inside conductivity value of 10^{-5} S/m. We see that the shape is reconstructed very well by the level set technique. Fig. 9 shows the reduction of the cost for the level set iteration during the first 12 steps of the shape reconstruction.

5 Conclusion

We have presented numerical results for tracking areas of frozen tissue in the brain for the application of cryosurgery. The main new feature of our method is the use of a level set technique for modeling propagating interfaces combined with an adjoint technique and a narrowband technique for calculating sensitivities for the shape evolution. The formulation of the underlying inverse problem as a shape reconstruction problem is well-suited to a high-contrast situation as the present one. We have presented a narrowband technique for calculating successive updates for an initially guessed level set function which results in a stable evolution scheme and which allows us to treat the shape reconstruction technique with quite similar tools as it is usually done for pixel or voxel based inverse problems. The evolving level set function corresponds to an evolving shape which quickly finds the correct location and size of the frozen material. Moreover, the narrowband technique allows us to use a fairly fine mesh for the inverse modeling without increasing dramatically the sizes of the subproblems to be solved in each step of the iterative reconstruction scheme. This has the effect of a better resolution power of our method. The computational effort in each step for calculating updates is concentrated on those areas where shape boundaries need to be refined. This

13

corresponds to the fact that we make implicitly use of the a-priori knowledge of the high contrast situation. No effort needs to be spent in order to recover this high contrast, which typically is a major bottleneck for traditional pixel or voxel based schemes. Our numerical experiments show that, by incorporating in addition very powerful forward solvers for the 3D EIT problem, we can achieve very good and stable reconstructions of the shapes of the frozen areas after only a few iterations of the proposed scheme.

In the following we list a few additional observations which convince us that the use of a level set technique for shape monitoring in cryosurgery from brain EIT data is a promising and powerful technique.

- Typically a good a-priori guess for the correct location of the ice-ball is available from knowledge of the location of the cryosurgery probes. Therefore, shape evolution with level sets is extremely fast in contrast to pixel-based schemes which still need many iterations for building up the high contrast in the conductivity values.

- The level set method leads to subproblems in each linearized step of the iteration which are much better posed and of smaller size than those which occur in pixel-based reconstruction schemes.

- As demonstrated in our previous work, the level set method works extremely well also when using experimental data.

- For large scale inverse problem such as brain EIT when there is a distinct phase difference it

could work well.

- The voltage change due to an ice-ball is detectable (it is in the mV range), so the actual monitoring of the ice-ball seems to be feasible.

- Due to the saturation property of the high contrast inverse problem as indicated in Fig. 7, the absolute conductivity values inside the ice-ball are hard to detect. On the other hand, beyond a given threshold value the actual choice of these values does not influence the data significantly: treating the objects as shapes with just one representative high or low conductivity value appears to be a reasonable approach.

- Our proposed method assumes a sharp change in conductivity between frozen and normal tissue. Accroding to **??**, the conductivity changes of the tissue behind the frozen tissue due to temprature drop needs to be taken into account. Our Tikhonov regularisation applied to the narrowband level set region applys some kind of smoothness into level set function (and consequently the coductivity of the narrowband region), but in our contiued study we need to consider this effect.

As future research we plan to further validate our model by using real data of ice-balls embedded in a brain-like phantom.

Acknowledgement

References

[1] K. Boone, A.M. Lewis and D.S. Holder, *"Imaging of cortical spreading depression by EIT: implications for localisation of epileptic foci*," Physiological Measurement, Institute of Physics, vol. 15, pp. A189-A198, 1994.

[2] Borsic A, McLeod C.N and Lionheart WRB, 2001, Total variation regularisation in EIT reconstruction 2nd World Congr. on Industrial Process Tomography (Hannover), 579 -587

[3] Breckon, W.R., 'Measurement and Reconstruction in EIT', Inverse Problems and Imaging, Research Notes in Mathematics 245, Ed Roach G., 130-140, Pitman, 1991.

[4] M.T. Clay and T.C. Ferree, *"Weighted regularization in Electrical Impedance Tomography with applicactions to acute cerebral stroke*," IEEE Transactions on Medical Imaging, vol. 21, no. 6, pp. 629-637, 2002.

[5] Chan T. F and Tai X-C. 2003 Identification of discontinuous coefficients in elliptic problems using total variation regulariation *SIAM J. Sci. Comput.* **25** (3) pp. 881–904.

[6] Chan T. F and Tai X-C. 2003 Level set and total variation regularization for elliptic inverse problems with discontinuous coefficients *J. Comput. Physics* **193** pp. 40–66.

[7] O. Dorn, E.L. Miller and C.M. Rappaport, *"A shape reconstruction method for electromagnetic tomography using adjoint fields and level sets,"* Inverse Problems, 16, pp. 1119-1156, 2000.

[8] O. Dorn, H. Bertete-Aguirre, J. G. Berryman and G. C. Papanicolaou, *"Sensitivity analysis of a nonlinear inversion method for 3D electromagnetic imaging in anisotropic media"*, Inverse Problems 18, pp. 285-317, 2002.

[9] J. F. Edd, L. Horwitz, B. Rubinsky, *Temperature Dependence of Tissue Impedivity in Electrical Impedance Tomography of Cryosurgery,* IEEE T BME, 52(4), pp. 695- 701, 2005.

[10] Ito K, Kunisch K and Li Z 2001 Level-set approach to an inverse interface problem *Inverse Problems* **17** pp 1225–1242

[11] A. Litman, D. Lesselier and F. Santosa, *"Reconstruction of a two-dimensional binary obstacle by controlled evolution of a level-set,"* Inverse Problems, 14, pp. 685-706, 1998.

[12] W.R.B. Lionheart, *"Reconstruction Algorithms for Permittivity and conductivity Imaging.,"* In Proc. 1th world congress on process tomography, Hannover, Germany, pp. 1-4, 2001.

17

[13] W Lionheart, N.Polydordes and A Borsic, The reconstruction problem, Part 1 of Electrical Impedance Tomography: Methods, History and Applications, (ed) D S Holder, Institute of Physics, p3-64, 2004.

[14] S. Osher and J. Sethian, *"Fronts propagation with curvature dependent speed: Algorithms based on Hamilton-Jacobi formulations,"* Journal of Computational Physics 56, pp. 12-49, 1988.

[15] S. Osher and R. Fedkiw, *"Level set methods and dynamic implicit surfaces"*, Springer, New York, 2003.

[16] N. Polydorides, W.R.B. Lionheart and H. McCann, *"Krylov subspace iterative techniques: On the detection of brain activity with EIT,"* IEEE T Medical Imaging, vol. 21, no. 6, pp. 596-603, 2002.

[17] N. Polydorides and W.R.B. Lionheart, *"A MATLAB based toolkit for three-dimensional electrical impedance tomography: A contribution to the EIDORS project,"* Measurement Science and Technology, Institute of Physics, vol. 13, no. 12, pp. 1871-1883, 2002.

[18] D.M. Otten and B. Rubinsky, *"Cryosurgical monitoring using bioimpedance measurements-A feasibility study for electrical impedance tomography.,"* IEEE T on BME, vol. 47, no. 10, pp. 1376-1381, 2000.

[19] D.M. Otten and B. Rubinsky, " *Front-tracking image reconstruction algorithm for EIT-monitored cryosurgery using the boundary element method,*" Physiol. Meas. 26, pp. 503-516, 2005

[20] M.M. Radai, S. Abboud and B. Rubinsky B, *"Evaluation of the impedance technique for cryosurgery in a theoretical model of the head,*" Cryobiology, vol. 38, no. 1, pp. 51-59, 1999.

[21] Rondi L and Santosa F, *"Enhaced electrical impedance tomography via the Mumford-Shah functional*, ESAIM: COCV 6, pp. 517-538, 2001.

[22] F. Santosa, *"A Level-Set Approach for Inverse Problems Involving Obstacles*," ESAIM: Control, Optimization and Calculus of Variations 1, pp. 17-33, 1996.

[23] J. A. Sethian, *"Level Set Methods and Fast Marching Methods*," (2nd ed) Cambridge University Press, 1999.

[24] M. Soleimani, W. R.B. Lionheart and O. Dorn, *"Level set reconstruction of conductivity and permittivity from boundary electrical measurements using experimental data,*" Inverse Problems in Science and Engineering, to appear.

[25] M. Soleimani, C.E. Powell and N. Polydorides, *"Improving the Forward Solver for the Complete Electrode Model in EIT using Algebraic Multigrid,*" IEEE T Medical imaging, vol. 24, issue 5, pp. 577-583, May 2005.

List of Figures
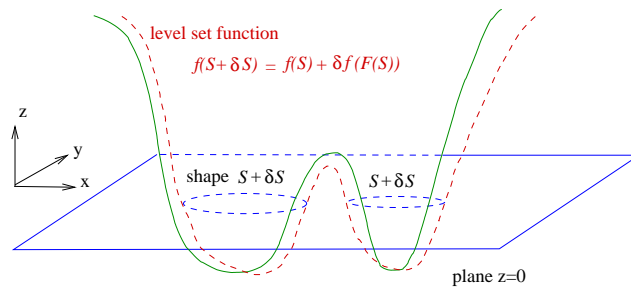
List of Tables

Figure 1: Perturbation of the level set function modeling the deformation of the shape by the velocity function $F(S)$.

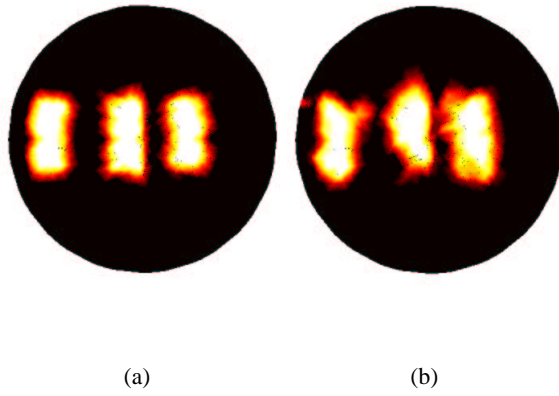(a)   (b)

Figure 2: Reconstruction of three inclusions with conductivity contrast from simulated data of an

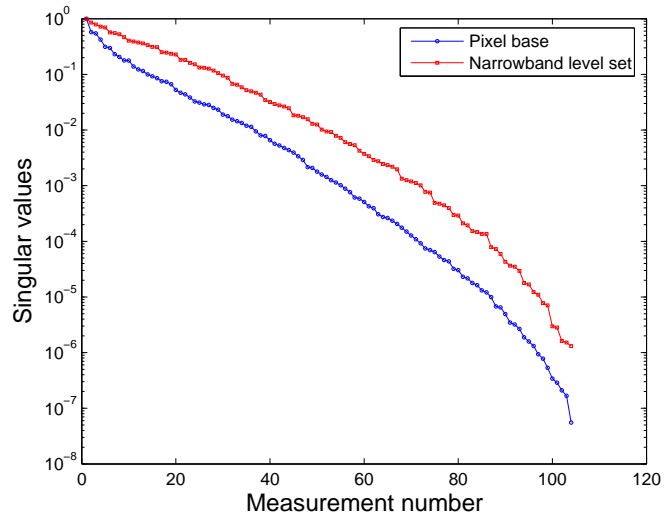16 electrode EIT system using the level set technique. True object (a) and reconstruction (b)

Figure 3: Singular values of the Jacobian in a logarithmic scale arising in the pixel based and the level set based scheme. Clearly visible is the difference of the condition numbers in these two schemes.
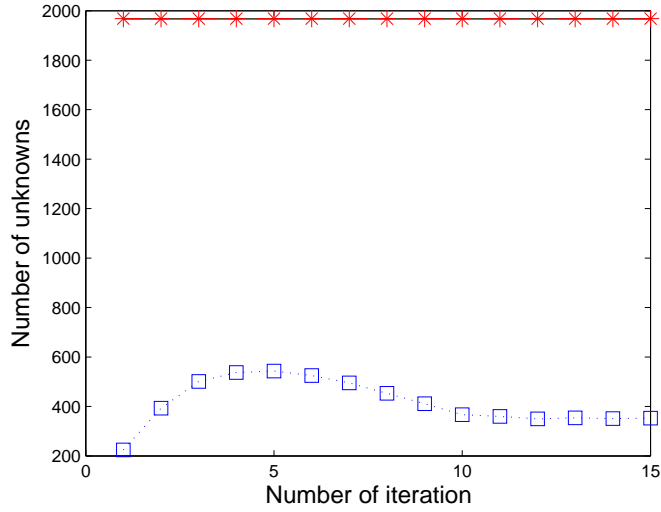
Figure 4: Reduction in number of unknowns in the linearized subproblems arising in each step of the iterative nonlinear reconstruction scheme. Boxes indicate values for the level set based scheme, and stars those for the pixel based scheme with roughly the same resolution. Notice that in the level set scheme this number depends on the actual narrow-band, and therefore on the actual boundary of the shape at a given iteration step.
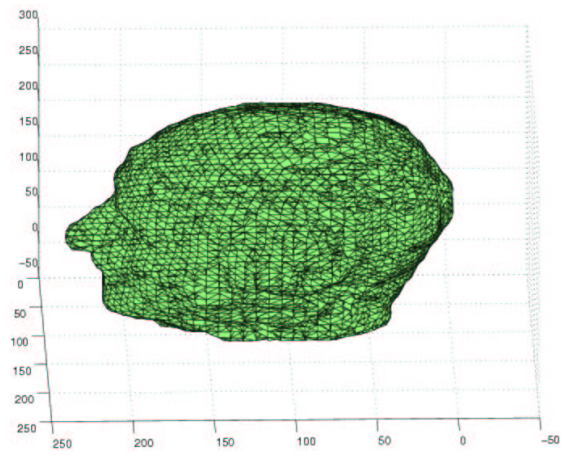
Figure 5: Arrangement of 16 surface electrodes at the surface of a head mesh, numbered anti-clockwise from above as indicated.
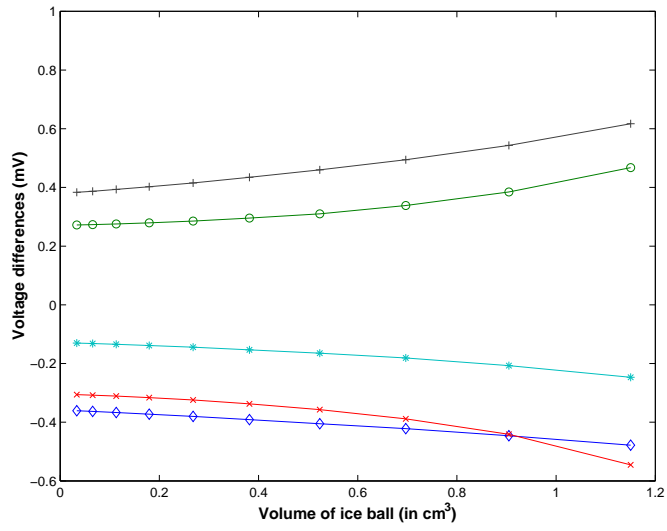
Figure 6: Voltage differences with respect to volume of the frozen region for several electrodes.
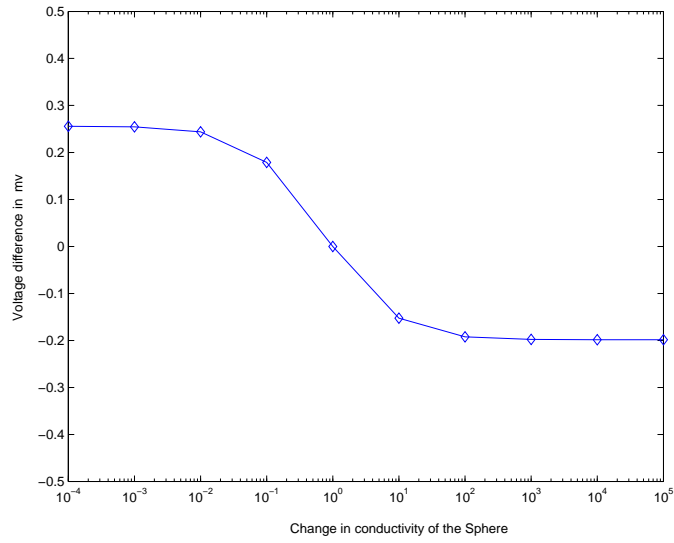
Figure 7: Displayed is the saturation behavior of the voltage difference at the electrodes due to large conductivity changes in a given region in the domain.
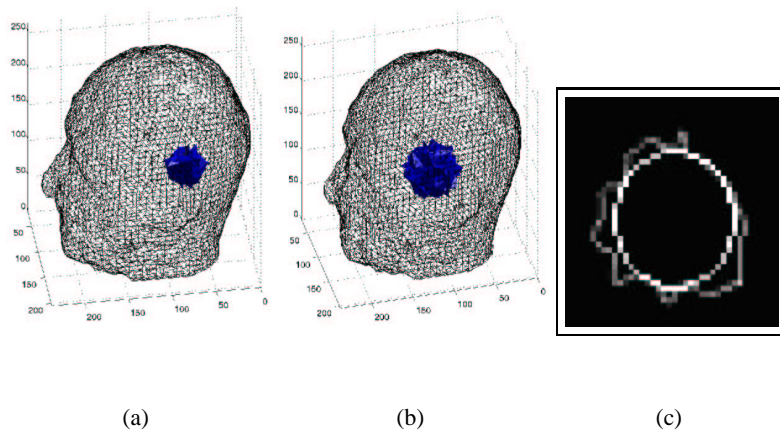
(a)　　　　　　　　　　(b)　　　　　　　　　　(c)

Figure 8: Two steps of the shape reconstruction with the level set method for monitoring and characterizing an ice-ball in the head for cryosurgery. (a): Initial guess, (b): shape after 10 iterations (b), and (c): To show the accuracy of the reconstructed image see the comparison between truth and reconstructed image iteration 6.
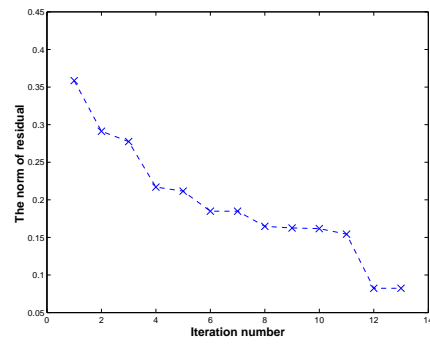
Figure 9: Evolution of the cost during the level set reconstruction for the test example of Fig. 8.

Table 1: Conductivity coefficients for the head model in Sm^{-1}

Tissue	Conductivity
scalp	0.172
skull	0.067
csf	1.540
gray matter	0.345
brain	0.150